

# Regulation of bacterial Type III Secretion System export gate opening by substrates and the FliJ stalk of the flagellar ATPase

Owain J. Bryant\* and Gillian M. Fraser 

Department of Pathology, University of Cambridge, UK

## Keywords

bacterial flagella biogenesis; protein export; Type III secretion

## Correspondence

G. M. Fraser and O. J. Bryant, Department of Pathology, University of Cambridge, Tennis Court Road, Cambridge CB2 1QP, UK

Tel: +44 1223 330245 (GMF);

+44 1223 366145 (OJB)

E-mails: gmf25@cam.ac.uk (GMF);

owain.bryant@bioch.ox.ac.uk (OJB)

## \*Present address

Department of Biochemistry, University of Oxford, UK

(Received 23 March 2021, revised 13 September 2021, accepted 22 November 2021)

doi:10.1111/febs.16294

Type III Secretion Systems (T3SS) transport proteins from the bacterial cytosol for assembly into cell surface nanomachines or direct delivery into target eukaryotic cells. At the core of the flagellar T3SS, the FlhAB-FliPQR export gate regulates protein entry into the export channel whilst maintaining the integrity of the cell membrane. Here, we identify critical residues in the export gate FliR plug that stabilise the closed conformation, preserving the membrane permeability barrier, and we show that the gate opens and closes in response to export substrate availability. Our data indicate that FlhAB-FliPQR gate opening, which is triggered by substrate export signals, is energised by FlhA in a proton motive force-dependent manner. We present evidence that the export substrate and the FliJ stalk of the flagellar ATPase provide mechanistically distinct, non-redundant gate-activating signals that are critical for efficient export.

## Introduction

Type III Secretion Systems (T3SS) transport proteins across the bacterial inner and outer membranes and, in the case of the virulence T3SS (vT3SS), across the plasma membrane of target eukaryotic cells [1–3]. The flagellar T3SS (fT3SS) is required for assembly of rotary flagella, which facilitate cell motility [1–4]. Despite their different functions, the vT3SS and fT3SS are evolutionarily related and contain conserved core export components [5–11].

For construction of the bacterial flagellum, most of the flagellar components are exported by the fT3SS machinery, which is embedded in the cell envelope.

The core of the export machinery is made up of five highly conserved proteins (FlhA, FlhB, FliP, FliQ and FliR). FlhA forms a nonameric ring comprising a cytoplasmic domain which functions as a docking platform for export cargo and an N-terminal region (FlhA<sub>N</sub>) with putative proton-conducting activity [5,12–14]. Recent cryo-ET data show that FlhA<sub>N</sub> wraps around the base of a helical-dome comprising FliPQR and the N-terminal region of FlhB (FlhB<sub>N</sub>) [13]. Together, FlhA and PQRB<sub>N</sub> constitute the ABPQR export gate, which regulates entry of flagellar subunits into the central channel that runs the length

## Abbreviations

Cryo-EM, cryogenic electron microscopy; fT3SS, flagellar type III secretion; kDa, kilodalton; M-gate, methionine gate; pmf, proton motive force; Q-latch, FliQ latch; R-plug, FliR plug; T3SS, type III secretion; vT3SS, virulence type III secretion.

of the nascent flagellum [5,12,13]. In addition to the ABPQR export gate, an ATPase complex (FliHIJ) located in the cytoplasm converts the  $\text{fT3SS}$  into a highly efficient pmf-driven protein export machine [10,15–17].

Recent structural studies of FliPQR and FlhB<sub>N</sub> have shown that multiple interactions stabilise the closed export gate [5,6,13,18]. A central plug formed by residues 106–120 of FliR, a methionine-rich loop (M-gate) within FliP, and ionic interactions between adjacent FliQ subunits maintain the closed conformation [5,6,18]. Structural analysis of the export gate in the open conformation revealed multiple rearrangements within the M-gate and an upward displacement of the FliR plug, indicating that energy must be provided to open the gate and permit subunit translocation across the inner membrane [18]. We reasoned that, as the PQRB components of the gate are positioned adjacent to the proposed proton-conducting FlhA membrane protein, FlhA might use the energy derived from the pmf to promote gate opening. Moreover, we hypothesised that gate opening must be regulated by one or more factors to permit subunit export whilst maintaining the membrane permeability barrier. We set out to test these hypotheses experimentally.

## Results

### Replacement of critical residues in the FliR plug destabilises the closed conformation of the $\text{fT3SS}$ export gate

The  $\text{fT3SS}$  ABPQR export gate resides in a closed conformation in the absence of subunit export [5,6,11,13,18]. We set out to engineer the export gate to destabilise the closed conformation and favour the open state, reasoning that mutation of contact points between adjacent gate subunits would reduce the energy barrier required for gate opening (Fig. 1A). To screen for potential gate opening mutants, we used an assembly-competent hook cap subunit variant (FlgD<sub>short</sub>) that we have previously shown is unable to trigger efficient opening of the export gate [19]. We predicted that mutations which promoted export gate opening would also suppress the motility defect associated with FlgD<sub>short</sub>. Recent structural information has revealed the potential gating mechanism of the FliPQR gate components. A region of FliR (residues 106–121) forms a plug that occludes the gate channel, and this plug must be displaced to achieve gate opening [18]. In the FliR plug, residues Phe-110 and Phe-113 make multiple contacts within the core of the export gate and might have a central role in gate opening [5,12].

To assess the importance of selected FliR residues in gate opening, we replaced Phe-110 and/or Phe-113 with alanine, and Gly-117 with a bulkier charged aspartate residue and screened for suppression of the FlgD<sub>short</sub> motility defect (Fig. 1B,C). We found that these FliR-plug mutations (F<sub>110</sub>A, F<sub>113</sub>A or G<sub>117</sub>D) suppressed the FlgD<sub>short</sub> motility defect, yet did not increase FlgD export or motility of cells encoding wild-type FlgD (Fig. 1B–G), suggesting these mutations promote export gate opening. The FliR-G<sub>117</sub>D mutation was previously proposed to rescue an interaction between FliR and FlhA, but the data presented here indicate that the G<sub>117</sub>D, F<sub>113</sub>A and F<sub>115</sub>A mutations directly destabilise the closed conformation of the export gate [20].

We hypothesised that deletion of the FliR plug would promote the open gate conformation and, as a result, increase the permeability of the inner membrane. Bacterial cells that fail to maintain the permeability barrier across the inner membrane are more sensitive to several chemical agents, including choline [21]. To determine whether a strain encoding a FliR plug deletion variant (FliR $\Delta$ 110–116, hereafter termed FliR $\Delta$ plug) was sensitive to choline, we performed growth inhibition assays by culturing cells in media containing increasing concentrations of choline. We found that the FliR $\Delta$ plug strain displayed wild-type export activity but was sensitised to choline compared to wild-type *Salmonella*, indicating that the FliR plug is important for formation of a tight barrier that is impermeable to small molecules, and for maintaining the closed conformation of the  $\text{fT3SS}$  export gate (Fig. 2A–E).

### The export gate fluctuates between open and closed states in response to substrate availability

A previous study showed the M<sub>210</sub>A mutation in the FliP component of the export gate sensitised cells to a variety of chemical agents [21]. This sensitivity could be reversed by trapping a subunit in the export channel, suggesting that the export gate can form an effective seal around a substrate during transit [21]. We reasoned that if the export gate fluctuates between open and closed conformations in response to the availability of substrate, strains producing fewer flagellar subunits would, at any given time, have fewer subunits transiting through the  $\text{fT3SS}$  to seal the leaky FliR $\Delta$ plug gate. To test this, we constructed a strain deleted for the genes that encode most of the early flagellar subunits by replacing a large portion of the *flg* operon (*flgB*, *flgC*, *flgD*, *flgE*, *flgF*, *flgG*, *flgH*, *flgI* and *flgJ*) with a kanamycin resistant cassette. An FlgE- $\beta$ -lactamase fusion was readily exported into the

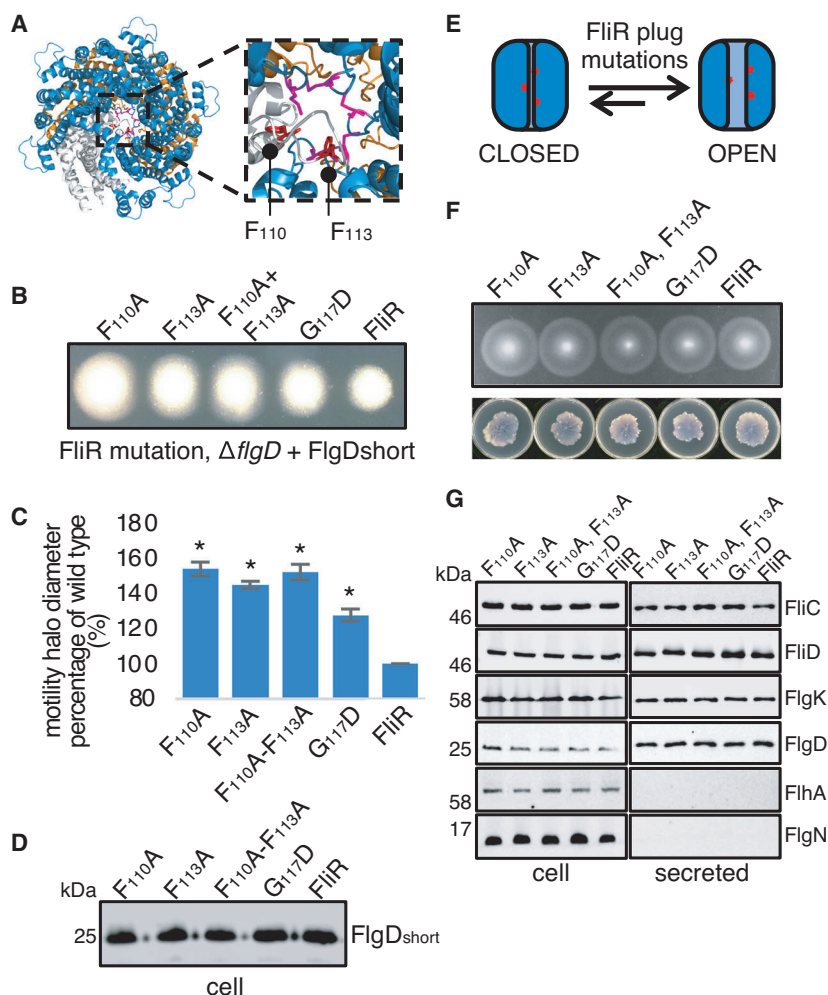


**Fig. 1.** Mutations within the FliR plug destabilise the closed export gate conformation. (A) Top view of the cryo-EM structure of the closed conformation of the FliPQR export gate complex (PDB:6F2D). Phenylalanine residues 110 and 113 of FliR (grey) are displayed in red. Methionine residue 210 of FliP (blue) is displayed in magenta. FliQ is displayed in orange. (B) Swimming motility of recombinant *Salmonella flgD* null strains producing chromosomally-encoded FliR variants (F<sub>110</sub>A, F<sub>113</sub>A, F<sub>110</sub>A+F<sub>113</sub>A or G<sub>117</sub>D) or wild-type FliR (FliR). Strains produced a pTrc99a plasmid-encoded FlgD subunit variant in which residues 9–32 were replaced with two repeats of the six amino acid sequence Gly-Ser-Thr-Asn-Ala-Ser (FlgD<sub>short</sub>). Motility was assessed in 0.25% soft-tryptone agar containing 100 μg·mL<sup>-1</sup> of ampicillin and 50 μM of IPTG and incubated at 37 °C for 16 h. (C) The mean motility halo diameter of recombinant *Salmonella flgD* null strains producing chromosomally-encoded FliR variants (F<sub>110</sub>A, F<sub>113</sub>A, F<sub>110</sub>A+F<sub>113</sub>A or G<sub>117</sub>D) or wild-type FliR (FliR) and expressing the FlgD<sub>short</sub> variant was plotted as a percentage of the wild-type FliR strain (FliR) producing FlgD<sub>short</sub> (right hand bar). Error bars represent the standard error of the mean calculated from at three biological replicates. \* indicates a *P*-value < 0.05. (D) Whole cell (cell) proteins from late exponential-phase cultures of recombinant *Salmonella flgD* null strains producing chromosomally-encoded FliR variants (F<sub>110</sub>A, F<sub>113</sub>A, F<sub>110</sub>A+F<sub>113</sub>A or G<sub>117</sub>D) or wild-type FliR (FliR), and a pTrc99a plasmid-encoded FlgD subunit variant in which residues 9–32 were replaced with two repeats of the six amino acid sequence Gly-Ser-Thr-Asn-Ala-Ser (FlgD<sub>short</sub>). Proteins were separated by SDS (15%)-PAGE and analysed by immunoblotting with anti-FlgD polyclonal antisera. Apparent molecular weights are in kilodaltons (kDa). (E) A cartoon schematic illustrating the effect of FliR plug mutations (red) on the conformation of the export gate complex (blue). Data indicates that FliR plug mutations destabilise the closed export gate conformation (left) and promote the open conformation (right). (F) Swimming (top panel; 0.25% soft tryptone agar) and swarming (bottom panels; 0.6% agar-tryptone with 0.5% glucose) motility of recombinant *Salmonella* strains producing chromosomally-encoded FliR variants (F<sub>110</sub>A, F<sub>113</sub>A, G<sub>117</sub>D or F<sub>110</sub>A+F<sub>113</sub>A) or SJW1103 wild-type (FliR). (G) Whole cell (cell) and secreted (secreted) proteins from late exponential-phase cultures of recombinant *Salmonella* strains producing chromosomally encoded FliR variants (F<sub>110</sub>A, F<sub>113</sub>A, G<sub>117</sub>D or F<sub>110</sub>A+F<sub>113</sub>A) or SJW1103 wild-type (FliR). Proteins were separated by SDS (15%)-PAGE and analysed by immunoblotting with anti-FliC, anti-FliD, anti-FlgK, anti-FlgD, anti-FliH and anti-FlgN polyclonal antisera. Apparent molecular weights are in kilodaltons (kDa).

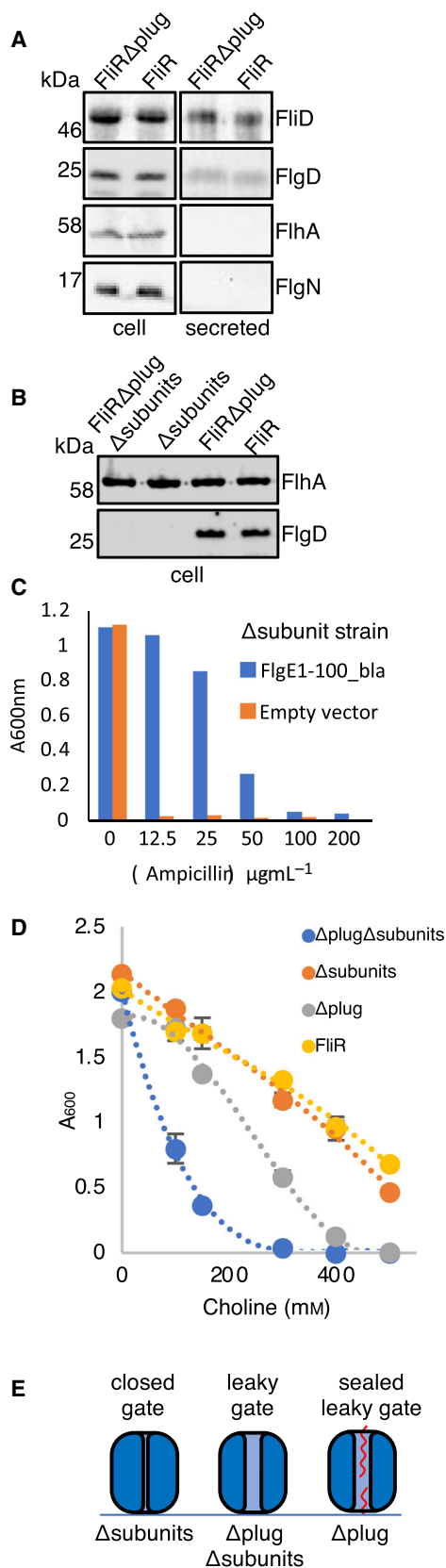


**Fig. 2.** FliR plug mutations that destabilise the closed export gate conformation sensitise cells to chemical agents. (A) Whole cell (cell) proteins from late exponential-phase cultures of recombinant *Salmonella* strains producing a chromosomally encoded FliR variant in which residues 110–116 of the FliR plug is deleted ( $\Delta$ plug), a *Salmonella* strain deleted for the genes (*flgBCDEFGHIJ*) that encode most of the early flagellar rod and hook subunits ( $\Delta$ subunits), a *Salmonella* strain that both produces the chromosomally-encoded FliR $\Delta$ plug variant and is deleted for the genes (*flgBCDEFGHIJ*) that encode most of the early flagellar rod and hook subunits ( $\Delta$ plug $\Delta$ subunits) and a SJW1103 wild-type strain (FliR) were separated by SDS (15%)-PAGE and analysed by immunoblotting with anti-FlhA and anti-FlgD polyclonal antisera. Apparent molecular weights are in kilodaltons (kDa). (B) Whole cell (cell) and supernatant (secreted) proteins from late exponential-phase cultures of a wild-type *Salmonella* strain (FliR) and a *Salmonella* strain producing a chromosomally-encoded FliR variant in which residues 110–116 of the FliR plug is deleted (FliR $\Delta$ plug). Proteins were separated by SDS (15%)-PAGE and analysed by immunoblotting with anti-FliC, anti-FliD, anti-FlgK, anti-FlgD, anti-FlhA or anti-FlgN polyclonal antisera. Apparent molecular weights are in kilodaltons (kDa). (C) Analysis of secretion by the *Salmonella*  $\Delta$ flgBCDEFGHIJ strain ( $\Delta$ subunit). The first 100 amino acids of FlgE were C-terminally fused to  $\beta$ -lactamase lacking its sec secretion signal. Cells expressing either the FlgE1-100  $\beta$ -lactamase fusion (FlgE1-100\_bla, blue) or carrying empty pBAD33 vector (Empty vector, orange) were grown to  $A_{600} = 1$  before being diluted 1 : 100 in LB containing the indicated concentration of ampicillin. The  $A_{600}$  of cultures was measured after 3.5 h incubation. (D) Choline sensitivity of a *Salmonella* strain producing a chromosomally encoded FliR variant in which residues 110–116 of the FliR plug is deleted ( $\Delta$ plug, grey), a *Salmonella* strain deleted for the genes (*flgBCDEFGHIJ*) that encode most of the early flagellar rod and hook subunits ( $\Delta$ subunits, orange), a *Salmonella* strain that both produces the chromosomally encoded FliR $\Delta$ plug variant and is deleted for the genes (*flgBCDEFGHIJ*) that encode most of the early flagellar rod and hook subunits ( $\Delta$ plug $\Delta$ subunits, blue) or a wild-type *Salmonella* strain (FliR, yellow). Cells were grown in Terrific broth containing varying concentrations of choline (as indicated) and the optical density ( $A_{600}$ ) measured following 4.5 h. (E) A cartoon schematic illustrating the effect of the FliR plug deletion on the gating activity of the export gate complex (blue). Strains that produce fewer subunits ( $\Delta$ subunits and  $\Delta$ plug $\Delta$ subunits) have fewer available subunits (red) for export to seal the leaky phenotype of the export gate containing the FliR plug deletion ( $\Delta$ plug, right).

periplasm of the  $\Delta$ subunit strain demonstrating that this strain is export competent (Fig. 2C). In addition, we constructed a second strain in which the FliR plug and the rod/hook genes were deleted. This FliR $\Delta$ plug- $\Delta$ subunit strain was significantly more sensitive to choline than the FliR $\Delta$ plug strain, indicating that transiting subunits partially seal the export gate when the FliR plug is absent (Fig. 2D–E). Notably, the  $\Delta$ subunit strain (which produces wild-type FliR) was not more sensitive to choline than wild-type *Salmonella*,

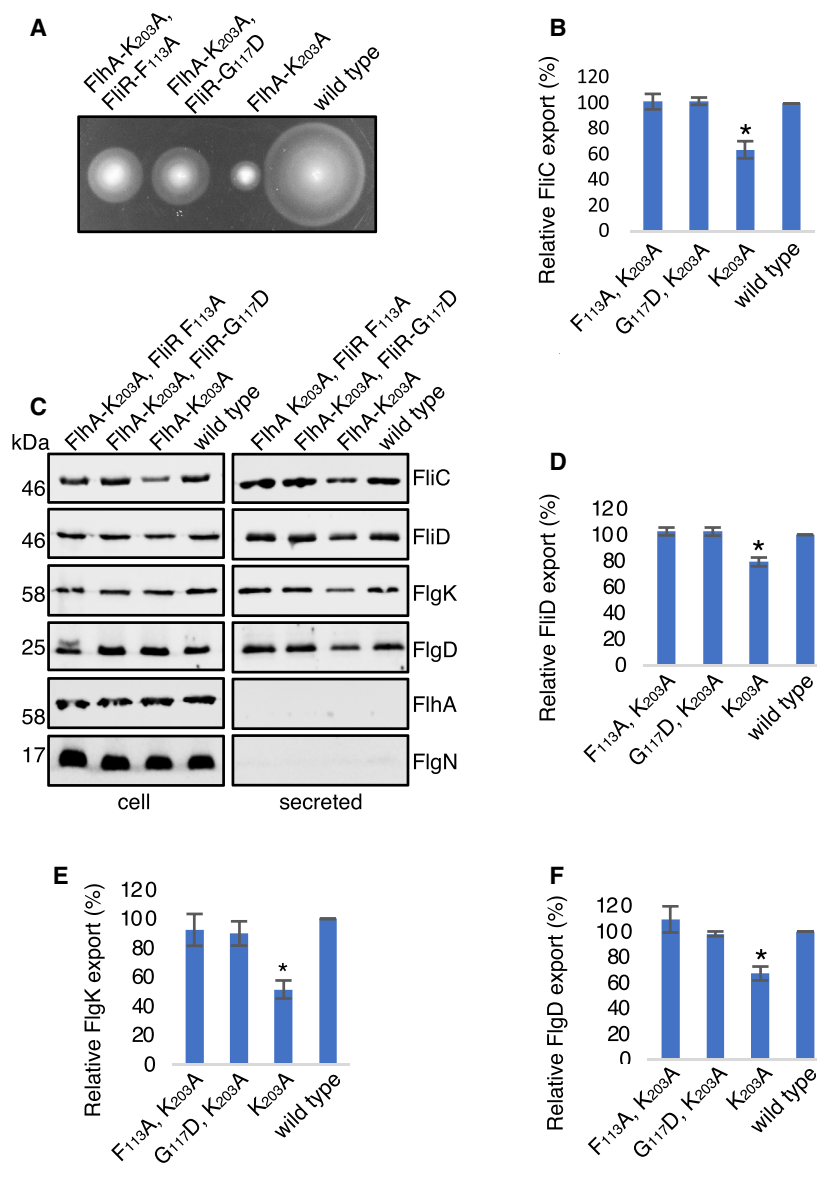


**Fig. 3.** Mutations in the FliR plug suppress the FlhA-K<sub>203</sub>A motility and export defects. (A) Swimming motility (0.25% soft tryptone agar) of a wild-type *Salmonella* strain, a *Salmonella* strain producing a chromosomally-encoded FlhA-K<sub>203</sub>A variant (FlhA K<sub>203</sub>A) or *Salmonella* strains producing both a chromosomally encoded FlhA-K<sub>203</sub>A variant and chromosomally encoded FliR variants (F<sub>113</sub>A or G<sub>117</sub>D) were carried out at 37 °C for 4–6 h. (b) Whole cell (cell) and supernatant (secreted) proteins from late exponential-phase cultures of the same strains. Proteins were separated by SDS (15%)-PAGE and analysed by immunoblotting with anti-FliC, anti-FliD, anti-FlgK, anti-FlgD, anti-FlhA or anti-FlgN polyclonal antisera. Apparent molecular weights are in kilodaltons (kDa). Levels of FliC (C), FliD (D), FlgK (E) and FlgD (F) in culture supernatants from Immunoblots were quantified using ImageStudioLite and plotted as a percentage of FlgK exported by the wild-type strain. Error bars represent the standard error of the mean calculated from three biological replicates. \* indicates a *P*-value < 0.05.

indicating that decreased subunit availability does not increase the permeability of the wild-type export gate to small molecules (Fig. 2D). This suggests that the export gate must fluctuate between open and tightly closed conformations in response to availability of subunits at the export machinery.

### Destabilising the closed conformation of the export gate alleviates the export defect associated with a variant of the gate component FlhA

Opening of the export gate is thought to be energised, in part, by harnessing of the pmf by FlhA. A previous

study proposed that FlhA interacts with FliR, as mutations in *fliR* were found to suppress the motility defect of a weakly motile *Salmonella* strain containing multiple flagellar gene mutations, including a point mutation in *flhA* K<sub>203</sub>W [20]. However, structural studies subsequently revealed that these FliR suppressor mutations are located in the core of the FliPQR complex, indicating that this region of FliR is unable to contact FlhA within the assembled  $\tau$ 3SS [5]. We have shown that one of these suppressor mutations in the FliR plug (FliR-G<sub>117</sub>D) destabilises the closed conformation of the export gate (Fig. 1B–C). Based on these data, we hypothesised that FliR-G<sub>117</sub>D might suppress the motility and export defects associated with

mutation of FlhA-K<sub>203</sub> by destabilising the closed conformation of the export gate, rather than by restoring an interaction between FliR and FlhA. To test this, we assessed whether the export and motility of strains encoding FlhA-K<sub>203</sub>A could be recovered by introducing mutations (FliR-F<sub>113</sub>A or FliR-G<sub>117</sub>D) that destabilise the closed gate conformation. We found that, as predicted, FliR-F<sub>113</sub>A and FliR-G<sub>117</sub>D suppressed the export and motility defects associated with FlhA K<sub>203</sub>A (Fig. 3). The data indicate that the *flhA*-K<sub>203</sub>A strain is unable to open the export gate efficiently and that introduction of *fliR* mutations that destabilise the closed gate might lower the energy barrier that must be overcome by FlhA-K<sub>203</sub>A to open the gate (Fig. 3A–F).

### Increasing the pmf suppresses the FlhA-K<sub>203</sub>A export defect

Our results support the view that FlhA has a role in opening the export gate and that FlhA-K<sub>203</sub> is critical for efficient gate opening. As FlhA has been proposed to facilitate subunit export by functioning as a proton-conducting channel [14,17,20], we hypothesised that the FlhA-K<sub>203</sub>A mutation might render the export machinery unable to couple pmf to efficient gate opening. If this were the case, the gate opening and subunit export defects of a strain carrying chromosomally encoded *flhA*-K<sub>203</sub>A might be overcome by increasing the pmf. To test this, we artificially increased the pmf across the bacterial inner membrane by driving intracellular proton consumption [22]. Cells supplemented with arginine convert intracellular protons and arginine to agmatine and CO<sub>2</sub> through the action of the cytoplasmic enzyme arginine decarboxylase, which effectively acts as a proton sink in the cytosol and therefore increases the pmf (Fig. 4A) [22]. We performed a modified subunit export assay in which cells were grown to mid-exponential phase, washed, resuspended in media containing 20 mM of arginine and culture supernatants were collected after 30 min. Addition of arginine to cultures of the *flhA*-K<sub>203</sub>A strain increased subunit export by 40%, whereas subunit export in the wild-type strain was unchanged (Fig. 4B,C). Deletion of the genes (*speA* and *adiA*) encoding the two *Salmonella* arginine decarboxylase enzymes abolished the arginine-dependent increase in subunit export in the *flhA*-K<sub>203</sub>A strain, indicating that the FlhA-K<sub>203</sub>A mutation prevented efficient use of the pmf by the export machinery. The data are consistent with wild-type FlhA utilising the pmf to energise export gate opening (Fig. 4D).

### Two distinct non-redundant signals activate the pmf-driven export machinery

We have found that the rod/hook subunit N-terminus contains a hydrophobic signal that triggers opening of the export gate [19], a process that would require an input of energy from either the flagellar ATPase and/or the proton motive force. We reasoned that the subunit ‘gate opening’ signal must somehow be transmitted to FlhA, triggering it to energise opening of the export gate. Previous studies have shown that, in addition, interaction of FlhA with the FliJ stalk component of the ATPase is required to convert the  $\Delta\psi$ SS into a highly efficient  $\Delta\psi$ -driven export machine, suggesting that the FliJ-FlhA interaction might be a second signal required for export gate opening [17]. Loss of either the FliJ-FlhA interaction or the subunit N-terminal hydrophobic signal can be overcome by suppressor mutations in the export machinery: FliH-FliI-FliJ loss can be bypassed by mutations in FlhA or FlhB [23,24], and we have shown that loss of the interaction between the FlgD<sub>short</sub> subunit N-terminal hydrophobic signal and the export machinery can be overcome by mutations in the genes encoding FliP or FliR that destabilise the export gate closed conformation [19]. We now wanted to test whether the suppressor mutations in the ABPQR export gate (FliR-F<sub>113</sub>A or FliR-G<sub>117</sub>D) that recovered export of FlgD<sub>short</sub> could also recover motility and export in strains deleted for the ATPase genes (in which the FliJ-FlhA interaction is lost; Fig. 5A,B). To test this, we constructed strains in which the chromosomal *fliR* gene was replaced with *fliR* alleles containing the gate opening mutations (F<sub>113</sub>A or G<sub>117</sub>D) in combination with deletions in the genes that encode the ATPase components FliH and FliI. These strains were also deleted for the gene encoding the flagellar anti-sigma factor FlgM, which is exported during the filament stage of assembly [25]. Deletion of *flgM* ensures that flagellar gene expression is not influenced by any differences in export efficiency between strains (Fig. 5) [26]. Mutations that promoted the open gate conformation (FliR-F<sub>113</sub>A or FliR-G<sub>117</sub>D) did not recover motility and export in strains deleted for the ATPase complex (Fig. 5A,B). This indicates that mutations that promote the open conformation of the FliPQR gate cannot bypass the loss of FliJ-dependent activation of FlhA.

We then assessed whether the FlhB-P<sub>28</sub>T suppressor, which enables bypass of flagellar ATPase activity (and, as a result, bypass of the requirement for the FliJ-FlhA interaction), could recover efficient gate opening by FlgD<sub>short</sub> (Fig. 5C). A *Salmonella flgD* null strain

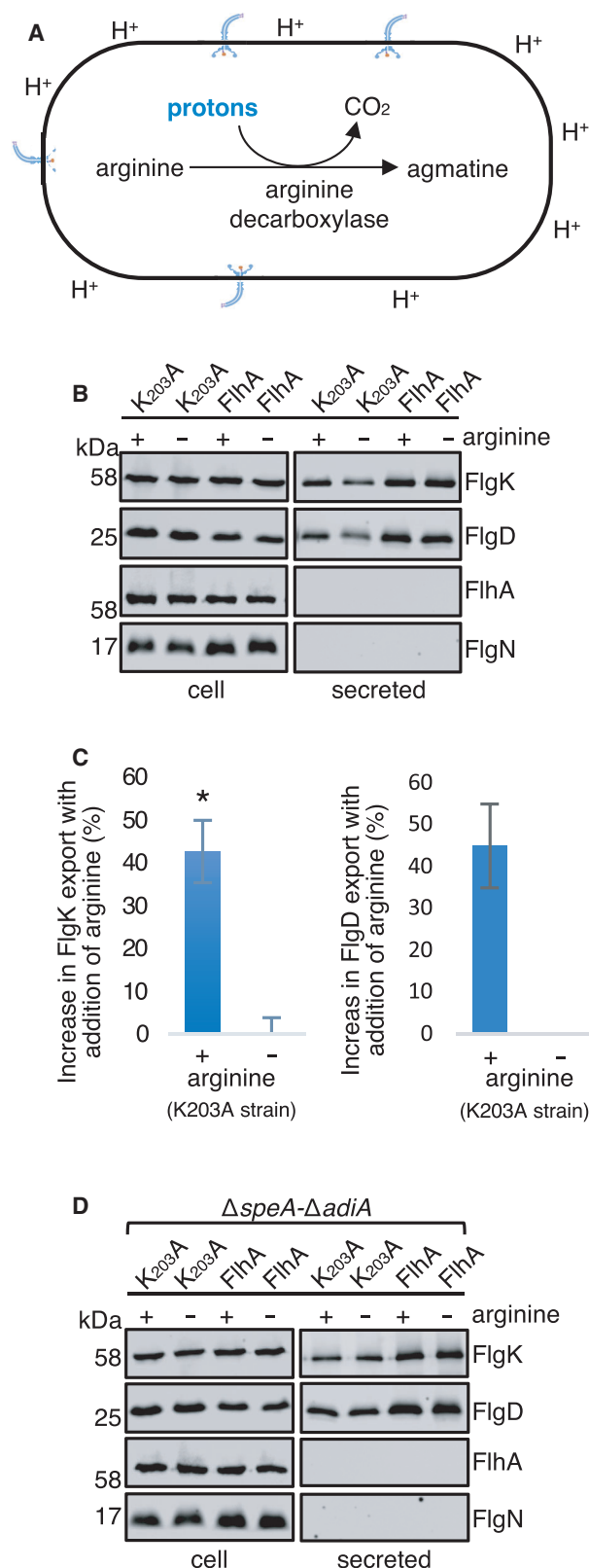


**Fig. 4.** Increasing the proton-motive force suppresses the *flhA*-K<sub>203</sub>A export defect. (A) A cartoon schematic of a cell containing arginine decarboxylase enzyme which catalyses the conversion of L-arginine into agmatine and carbon dioxide (CO<sub>2</sub>). The arginine decarboxylation reaction consumes a proton (H<sup>+</sup>) from the cell cytoplasm, reducing the number of protons in the cell, effectively increasing the proton-motive force. (B) Whole cell (cell) and supernatant (secreted) proteins from late exponential-phase cultures of a wild-type *Salmonella* strain (FlhA) or a *Salmonella* strain producing a chromosomally encoded FlhA-K<sub>203</sub>A variant (K<sub>203</sub>A). Cells were supplemented with (+) or not supplemented with (-) 20 mM of arginine 30 min prior to collection of whole cell and culture supernatants. Proteins were separated by SDS (15%)-PAGE and analysed by immunoblotting with anti-FlgK, anti-FlgD, anti-FlhA or anti-FlgN polyclonal antisera (Left). Apparent molecular weights are in kilodaltons (kDa). (C) Levels of FlgK (left) or FlgD (right) in culture supernatants from Immunoblots for the FlhA-K<sub>203</sub>A strain were quantified using ImageStudioLite and plotted as a percentage of FlgK exported by strains supplemented with arginine (+) to strains not supplemented with arginine (-) (right). Error bars represent the standard error of the mean calculated from three biological replicates. \* indicates a *P*-value < 0.05. (D) Whole cell (cell) and supernatant (secreted) proteins from late exponential-phase cultures of a strain deleted for two genes that encode arginine decarboxylase enzymes ( $\Delta$ *speA* and  $\Delta$ *adiA*, labelled FlhA) or a *Salmonella*  $\Delta$ *speA*- $\Delta$ *adiA* strain producing a chromosomally-encoded FlhA-K<sub>203</sub>A variant (K<sub>203</sub>A). Cells were supplemented with (+) or not supplemented with (-) 20 mM of arginine 30 min prior to collection of whole cell and culture supernatants. Proteins were separated by SDS (15%)-PAGE and analysed by immunoblotting with anti-FlgK, anti-FlgD, anti-FlhA or anti-FlgN polyclonal antisera. Apparent molecular weights are in kilodaltons (kDa).

encoding *flhB*-P<sub>28</sub>T and producing FlgD<sub>short</sub> was found to be no more motile than the parental *Salmonella* *flgD* null strain producing FlgD<sub>short</sub> (Fig 5C). This indicates that the FlhB-P<sub>28</sub>T mutation does not promote opening of the export gate, but instead restores fT3SS activity in the absence of the FliJ activation signal by an alternative mechanism (Fig. 5C).

These data indicate that mutations in *fliP* or *fliR* that promote the open conformation of the export gate and mutations that bypass the need for the FliJ-FlhA interaction are unable to compensate for each other, indicating that the subunit N-terminal hydrophobic export signal and the FliJ-FlhA interaction signal are non-redundant, that is both signals are required to activate pmf-driven opening of the ABPQR export gate by FlhA (Fig. 5).

## Discussion

Transport of substances across the bacterial inner membrane is highly selective, thereby maintaining the

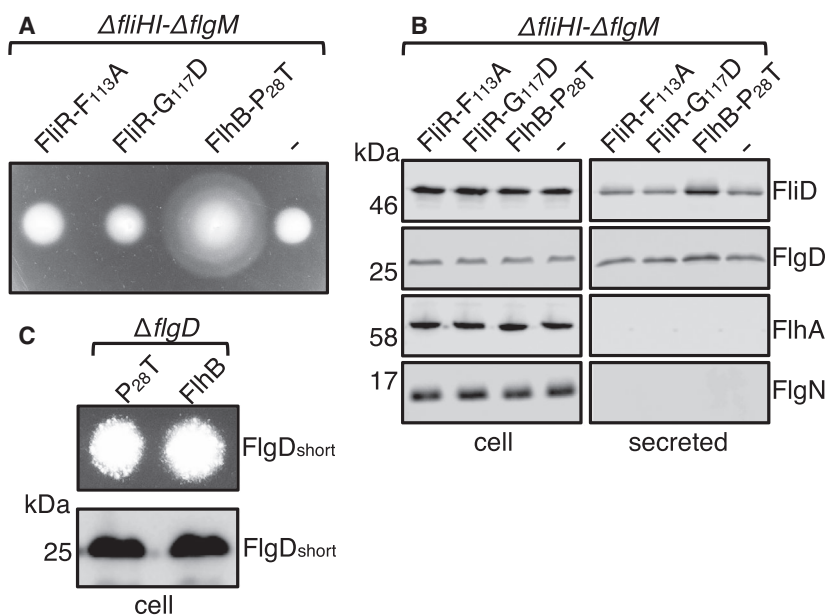


**Fig. 5.** Mutations in the FliR plug do not suppress export and motility defects of strains deleted for the ATPase complex. (A) Swimming motility of recombinant *Salmonella* strains deleted for the genes that encode; the anti-sigma(28) factor (*flgM*), the flagellar ATPase negative regulator (*fliH*) and the flagellar ATPase subunit (*fliI*) and producing either a chromosomally encoded FliB-P<sub>28</sub>T variant or producing chromosomally encoded wild-type FliR (-) or its variants (F<sub>113</sub>A or G<sub>117</sub>D). Motility was assessed in 0.25% soft-tryptone agar and incubated at 37 °C for 4–6 h. (B) Whole cell (cell) and supernatant (secreted) proteins from late exponential-phase cultures of the same strains were separated by SDS (15%)-PAGE and analysed by immunoblotting with anti-FliD, anti-FlgD, anti-FlhA or anti-FlgN polyclonal antisera. Apparent molecular weights are in kilodaltons (kDa). (C) Swimming motility (top) of recombinant *Salmonella* *flgD* null strains producing chromosomally-encoded wild-type FliB (FliB) or its variants (FliB-P<sub>28</sub>T). Both strains produced a pTrc99a plasmid-encoded FlgD subunit variant in which residues 9–32 were replaced with two repeats of the six amino acid sequence Gly-Ser-Thr-Asn-Ala-Ser (FlgD<sub>short</sub>). Motility was assessed in 0.25% soft-tryptone agar containing 100  $\mu\text{g}\cdot\text{mL}^{-1}$  of ampicillin and 50 of  $\mu\text{M}$  IPTG and incubated at 37 °C for 16 h. Whole cell (cell) fractions from late exponential-phase cultures of the same strains. Proteins were separated by SDS (15%)-PAGE and analysed by immunoblotting with anti-FlgD polyclonal antisera (bottom). Apparent molecular weights are in kilodaltons (kDa).

essential electrochemical gradients that drive numerous processes at the cell membrane, including ATP synthesis and protein export. The  $\sigma^{28}$  translocates proteins efficiently across the inner membrane without compromising the permeability barrier [5,18,21]. The ABPQR flagellar export gate contains three constriction points that are proposed to maintain the gate in a closed conformation, preserving the integrity of the membrane permeability barrier [5]. Here, we identified point mutant and deletion variants of proteins in the ABPQR export gate that destabilise its closed conformation. We show that either by destabilising the export gate closed conformation or by increasing the pmf, the flagellar export defects of strains encoding FliA-K<sub>203</sub>A can be alleviated, indicating that FliA harnesses the pmf to energise opening of the export gate complex. Additional *in vivo* experiments revealed that FliA requires activation by both the flagellar ATPase stalk component FliJ and an N-terminal hydrophobic signal in the export substrate to trigger efficient gate opening and subunit export.

### Mutational analysis of the FliR-plug identifies variants that destabilise the closed conformation of the export gate

Structures of the FliPQR export gate have revealed that, in the absence of the export substrate, multiple non-covalent interactions in the gate complex stabilise the closed conformation [5,13,18]. In particular, a 15-residue region of FliR forms a plug that occludes the central channel of the gate. Two residues within the FliR-plug, FliR-F<sub>113</sub> and FliR-F<sub>115</sub>, interact with a concentric ring of conserved methionine residues (M-gate) in FliP [5]. Our mutational analyses identified FliR variants, FliR-F<sub>113</sub>A and FliR-F<sub>115</sub>A, that destabilise the closed conformation of the export gate [5], indicating that these residues help to maintain the gate in its closed state in the absence of export substrate. An additional FliR-plug variant, FliR-G<sub>117</sub>D, also destabilised the closed gate, suggesting that the introduction of a bulky, charged side chain at this site prevents tight closure of the gate. A recent structure of

the open export gate revealed multiple rearrangements within the M-gate and an upward displacement of the FliR plug to allow subunit passage [18]. This indicates that the FliR plug, which occludes the export channel in the closed gate conformation, must be displaced to allow passage of unfolded subunits through the gate. A strain containing a deletion within the FliR-plug (residues 110–116) displayed choline sensitivity, consistent with the plug forming a tight seal to maintain the membrane permeability barrier (Fig 2). Notably, we found that a FliR-plug deletion strain that produced fewer subunits was significantly more sensitive to choline than a strain that encoded wild-type FliR and produced fewer subunits (Fig 2). An FlgE- $\beta$ -lactamase fusion was readily exported into the periplasm of the strain encoding fewer subunits ( $\Delta$ subunit strain), as assessed by determining the minimum inhibitory ampicillin concentration (MIC) which was comparable to the MIC observed by others (Fig. 2C) [27].

These data indicate that (a) subunit transit through the export gate can partially rescue the choline-sensitive phenotype associated with loss of the FliR-plug, and (b) that when no subunits available for transit, the wild-type export gate closes to maintain the membrane permeability barrier. These observations have important implications for our understanding of how the export gate opens. Sequential rounds of gate opening and closing must occur in response to the presence or absence of export substrates at the membrane export machinery. Similar gating mechanisms have been observed in other protein-conducting channels, such as the SecY channel, which similarly contains a constriction formed by ring of hydrophobic residues and a central plug that forms a seal [28]. Deletion of either the central plug or the ring of hydrophobic residues in SecY results in increased permeability of the channel, and electrophysiology experiments showed that these deletions cause the channel to alternate between an open and closed state [29]. Furthermore, molecular dynamic simulations indicate that the force required for opening the gate is reduced in SecY plug deletion mutants [30]. We found that deletion of the FliR plug similarly destabilised the closed conformation of the export gate and concomitantly increased permeability of the inner membrane (Fig. 2).

### FlhA activity is required for efficient opening of the export gate

A previous study identified suppressor mutations in the gene encoding FliR that rescued the export defect of a strain that contained mutations in *flhA* (K<sub>203</sub>W) and *flhB* (P<sub>28</sub>T), as well as deletions in the genes

encoding flagellar export ATPase components (*fliH* and *fliI*) [20]. The authors proposed that the FliR suppressor mutations might recover an interaction between FliR and FlhA [20]. One of these suppressor mutations (FliR-G<sub>117</sub>D) is positioned within the core of the FliPQR complex and introduces a bulky, charged side chain into the lumen of the export gate. We showed that the FliR-G<sub>117</sub>D mutation partially suppressed the motility defect associated with a subunit (FlgD<sub>short</sub>) that is unable to trigger efficient opening of the export gate, indicating that the FliR-G<sub>117</sub>D mutation might instead destabilise the export gate's closed conformation (Fig. 1B,C). We hypothesised that by the same mechanism, the FliR-G<sub>117</sub>D mutation might also suppress the motility and export defects associated with FlhA-K<sub>203</sub>. *Salmonella* strains carrying the *flhA*-K<sub>203</sub>A mutation in combination with mutations in *fliR* (F<sub>113</sub>A or G<sub>117</sub>D), which destabilise the closed conformation of the export gate, displayed enhanced flagellar export and motility compared to the parental *Salmonella flhA*-K<sub>203</sub>A strain (Fig. 3). This indicates that *FlhA*-K<sub>203</sub>A is unable to facilitate efficient export gate opening and, as a result, attenuates subunit export and cell motility.

Cryo-electron tomograms of the *Salmonella* injectisome have revealed that the FlhA homologue, InvA, is positioned adjacent to the homologues of the FliPQR export gate components, SpaPQR [13]. As FlhA is proposed to function as a proton-conducting channel that energises export, we reasoned proton translocation might be coupled to gate opening, possibly through transmission of conformational changes in FlhA to the adjacent FliPQR-FlhB components of the export gate [13,14,20]. In support of this view, we found that by increasing the pmf across the inner membrane, through supplementation of cell cultures with arginine, subunit export by the *flhA*-K<sub>203</sub>A strain could be enhanced by 40%, suggesting that inefficient export in the *flhA*-K<sub>203</sub>A strain is caused by its decreased ability to couple the pmf to gate opening (Fig. 4).

### Two distinct signals activate the pmf-driven export machinery

Previous studies have shown that the FliJ stalk component of the flagellar ATPase interacts with FlhA to convert the export machinery into a highly efficient  $\Delta\psi$ -driven export machine [17,31–33]. The FliH and FliI components of the ATPase facilitate the FliJ-FlhA interaction to promote full activation of the export gate [13,32]. These findings indicate that FliJ binding to FlhA modulates its proton conducting ability,

analogous to the interactions between the stalk component of the  $F_1$  ATPase and the membrane-localised  $F_0$  channel that drive proton translocation across the bacterial inner membrane. The need for activation of FlhA by the FliJ stalk, to facilitate efficient use of the  $\Delta\psi$  component of the pmf and energise gate opening, can be bypassed by mutations in *flhA* and *flhB* that overcome the loss of the flagellar ATPase [8,23,24].

In addition to the FliJ-dependent gate opening signal, we have previously shown that a subunit N-terminal hydrophobic signal is required to trigger opening of the export gate (Fig. 1B) [19]. To determine whether both signals were required to trigger opening of the export gate or whether the signals were functionally redundant, we asked if suppressor mutations in the ABPQR export gate (FliR-F<sub>113</sub>A or FliR-G<sub>117</sub>D) that could compensate for loss of the subunit N-terminal hydrophobic signal could also overcome loss of the flagellar ATPase (and of the FliJ-dependent gate opening signal). We found that neither FliR-F<sub>113</sub>A nor FliR-G<sub>117</sub>D could suppress the export defect caused by the loss of FliJ-dependent activation

of FlhA (Fig. 5). Taking the reciprocal approach, we found that a mutation in *flhB* (P<sub>28</sub>T) that alleviates the loss of the FliJ-dependent activation signal could not overcome loss of the subunit N-terminal hydrophobic signal (Fig 5). This indicates that both signals are essential for efficient opening of the flagellar export gate. We propose that FliJ binding to FlhA and the presence of a subunit at the export machinery induce distinct conformational changes in FlhA, rendering the export machinery competent to utilise the pmf to energise opening of the export gate. The lack of either signal prevents opening of the export gate and, in turn, maintains the membrane permeability barrier (Fig. 6).

Based on the structural and functional similarities between the core components of the injectisome and flagellar Type III Secretion Systems, it is highly probable that the mechanism of export gate opening is conserved. In summary, we propose that the pmf induces conformational changes in FlhA that are transmitted to the adjacent FliPQR-FlhB<sub>N</sub> components of the export gate, energising gate opening. We demonstrate that FlhA requires at least two distinct signals to

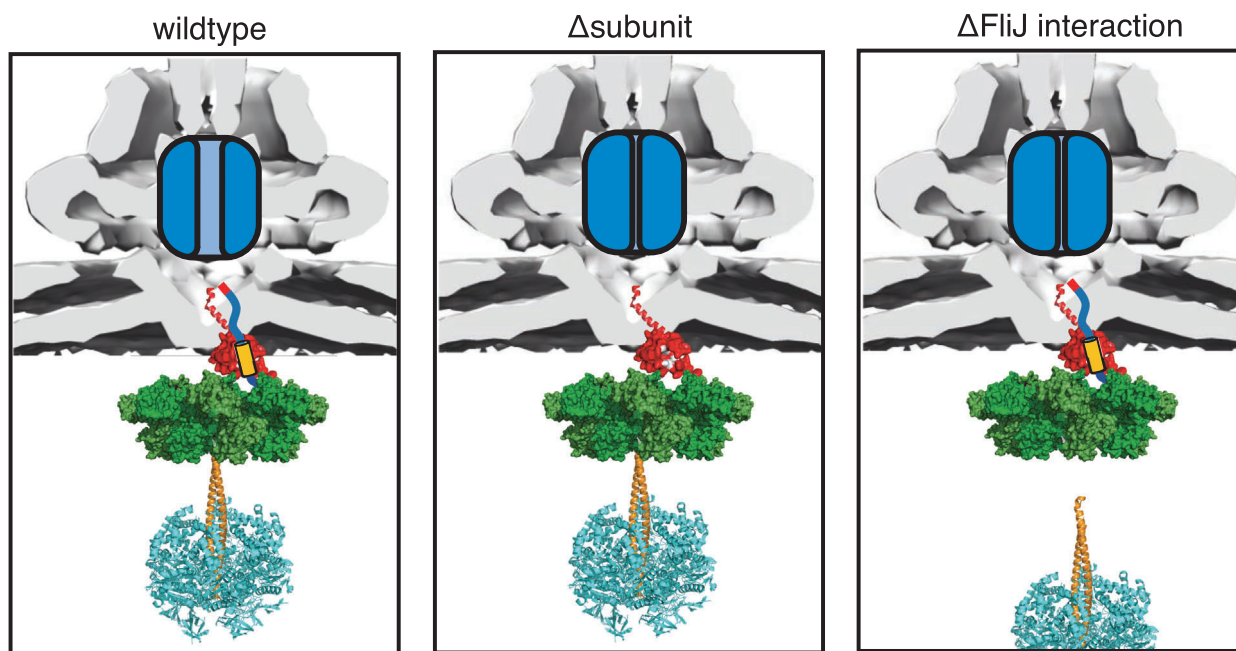


**Fig. 6.** Two mutually exclusive signals are required to activate the export machinery and trigger opening of the export gate. A cartoon schematic illustrating the effect of either (a) the absence of subunits docked at the export machinery (middle,  $\Delta$ subunit) or (b) the absence of a FliJ-FlhA interaction (right,  $\Delta$ FliJ) (required to convert the export machinery into a highly efficient  $\Delta\psi$ -driven export machine) on the ability of the export machinery to energise export gate opening (blue). ATP hydrolysis by the FliI (orange, PDB: 2DPY) component of the ATPase complex is thought to drive rotation of the FliJ stalk subunit (orange, PDB: 3AJW), allowing FliJ to bind all nine binding sites on the nonameric ring of FlhA (green, PDB: 3A5I), converting the export machinery into a highly efficient  $\Delta\psi$ -driven export machine. Early flagellar subunits dock at FlhBc (red, PDB: 3B0Z) and contain a N-terminal hydrophobic export signal required for efficient subunit export and translocation through the export gate complex (left). The absence of subunits at the export machinery (middle) or the absence of FliJ-FlhA interactions (right) renders the export machinery unable to utilise the PMF to drive opening of the export gate.

facilitate subunit export: a FliJ-dependent activation signal and a subunit docked at the export machinery. Our data suggest a multi-signal control system that acts *via* FlhA to ensure that use of the pmf and export gate opening only occurs when a FliJ activation signal is received and a subunit is available for export.

## Materials and methods

### Bacterial strains, plasmids and growth conditions

*Salmonella* strains and plasmids used in this study are listed in Table 1. The  $\Delta flgD::K_m^R$  strain in which the *flgD* gene was replaced by a kanamycin resistant cassette and the  $\Delta flgBCDEFGHIJ::K_m^R$  strain in which a large portion of the *flg* operon was replaced with a kanamycin cassette were constructed using the  $\lambda$  Red recombinase system [34–35]. Strains containing chromosomally encoded FliR and/or FlhA variants were constructed by aph-I-SceI Kanamycin resistant cassette replacement using pWRG730 [35]. Recombinant proteins were expressed in *Salmonella* from isopropyl  $\beta$ -D-thiogalactoside-inducible (IPTG) inducible plasmid pTrc99a [36]. Bacteria were cultured at 30–37 °C in Luria-Bertani (LB) broth containing ampicillin (100  $\mu\text{g}\cdot\text{mL}^{-1}$ ).

### Choline sensitivity assay

The choline sensitivity assay was performed essentially as described in Ward *et al.* [21]. Cells were grown overnight at 32 °C in terrific broth (TB) medium with shaking (200 r.p.m.). The overnight cultures were diluted 1 : 50 in TB and grown at 32 °C with shaking (200 r.p.m.) to an  $A_{600}$  1.0. These cultures were diluted 1 : 50 in TB containing choline at concentrations as indicated in Fig. 2. The cultures were grown for 4.5 h at 32 °C with shaking (200 r.p.m.) and the  $A_{600}$  measured. The Miles and Misra method [37] was used to determine the colony forming units for strains grown in 300 mM of choline. Ten-fold dilutions of culture were spotted (10  $\mu\text{L}$ ) onto LB agar plates and grown overnight at 37 °C.

### Flagellar subunit export assay

*Salmonella* strains were cultured at 37 °C in LB broth containing ampicillin and IPTG to mid-log phase ( $A_{600\text{ nm}}$  0.6–0.8). Cells were centrifuged (6000 *g*, 3 min) and resuspended in fresh media and grown for a further 60 min at 37 °C. Cells were pelleted by centrifugation (16 000 *g*, 5 min) and the supernatant passed through a 0.2  $\mu\text{m}$  nitrocellulose filter. Proteins were precipitated with 10% trichloroacetic acid (TCA) and 1% Triton-X100 on ice for 1 h, pelleted by centrifugation (16 000 *g*, 10 min), washed with ice-cold acetone and resuspended

**Table 1.** Strains and recombinant plasmids.

Strains	Description
<i>Salmonella typhimurium</i>	
SJW1103	Wild type
<i>flgD</i> null	$\Delta flgD::\text{kmR}$
<i>fliR</i> (F110A)	<i>fliR</i> F110A variant
<i>fliR</i> (F113A)	<i>fliR</i> F113A variant
<i>fliR</i> (F110A,F113A)	<i>fliR</i> F110A,F113A variant
<i>fliR</i> (G117D)	<i>fliR</i> G117D variant
<i>fliR</i> (F110A), <i>flgD</i> null	<i>fliR</i> F110A variant, $\Delta flgD::\text{kmR}$
<i>fliR</i> (F113A), <i>flgD</i> null	<i>fliR</i> F113A variant, $\Delta flgD::\text{kmR}$
<i>fliR</i> (F110A,F113A), <i>flgD</i> null	<i>fliR</i> F110A, F113A variant, $\Delta flgD::\text{kmR}$
<i>fliR</i> (G117D), <i>flgD</i> null	<i>fliR</i> G117D variant, $\Delta flgD::\text{kmR}$
<i>fliR</i> ( $\Delta$ 110-116)	<i>fliR</i> $\Delta$ 110-116 variant
<i>fliR</i> ( $\Delta$ 110-116), <i>flgBCDEFGHIJ</i> null	<i>fliR</i> $\Delta$ 110-116 variant, $\Delta flgBCDEFGHIJ::\text{KmR}$
<i>flhA</i> (K203A)	$\Delta flgBCDEFGHIJ::\text{K mR}$
<i>flhA</i> (K203A), <i>fliR</i> (F113A)	<i>flhA</i> K203A variant
<i>flhA</i> (K203A), <i>fliR</i> (G117D)	<i>flhA</i> K203A variant, <i>fliR</i> F113A variant
<i>flhA</i> (K203A), <i>adiA</i> null, <i>speA</i> null	<i>flhA</i> K203A variant, <i>fliR</i> G117D variant
<i>adiA</i> null, <i>speA</i> null	<i>flhA</i> K203A variant, $\Delta adiA::\text{KmR}$ , $\Delta speA::\text{SpectR}$
<i>fliR</i> (F113A), <i>fliHI</i> null, <i>flgM</i> null	$\Delta adiA::\text{KmR}$ , $\Delta speA::\text{SpectR}$
<i>fliR</i> (G117D), <i>fliHI</i> null, <i>flgM</i> null	<i>fliR</i> F113A variant, $\Delta fliHI$ , $\Delta flgM::\text{SpectR}$
<i>flhB</i> (P28T), <i>fliHI</i> null, <i>flgM</i> null	<i>fliR</i> G117D variant, $\Delta fliHI$ , $\Delta flgM::\text{SpectR}$
<i>fliHI</i> null, <i>flgM</i> null	<i>flhB</i> P28T variant, $\Delta fliHI$ , $\Delta flgM::\text{SpectR}$
<i>flhB</i> (P28T), <i>flgD</i> null	$\Delta fliHI$ , $\Delta flgM::\text{SpectR}$
<i>flhB</i> (P28T), <i>flgD</i> null	<i>flhB</i> P28T variant, $\Delta flgD::\text{KmR}$
Plasmids	
pTrc99a FlgD	1-232aa
pTrc99a FlgD <sub>short</sub>	1-8, Gly, 2x(Gly- Ser-Thr-Asn-Ala- Ser), 33-232aa
pWRG730	Lambda red recombinase under the PL promoter under the control of the temperature sensitive C1857 repressor. I-SceI under the Tet promoter.
pWRG717	Kanamycin resistant cassette with I-SceI recognition site

in SDS-PAGE loading buffer (volumes calibrated according to cell densities). Fractions were analysed by immunoblotting. For the export assays of strains supplemented with arginine, cells were treated essentially as described above except cells were resuspended in fresh media supplemented with 20 mM of arginine and grown for further 30 min instead of 60 min.

### Motility assays

For swimming motility, cultures were grown in LB broth to  $A_{600\text{ nm}}$  1. Two microlitres of culture were inoculated

into soft tryptone agar (0.3% agar, 10 g·L<sup>-1</sup> of tryptone, 5 g·L<sup>-1</sup> of NaCl) containing ampicillin (100 µg·mL<sup>-1</sup>). Plates were incubated at 37 °C for between 4 and 6 h unless otherwise stated. For swarming motility, 1 µL of overnight culture grown in LB broth was inoculated onto tryptone agar plates (0.6% agar, 1% w/v tryptone, 0.5% w/v sodium chloride) containing appropriate antibiotics and inducing agents and supplemented with 0.3% glucose and incubated at 30 °C for 12–16 h.

### β-lactamase secretion assay

Cultures were grown in LB broth containing chloramphenicol (20 µg·mL<sup>-1</sup>) to A<sub>600 nm</sub> 1. Cultures were diluted 1 : 100 in fresh media containing chloramphenicol (20 µg·mL<sup>-1</sup>) supplemented with increasing concentrations of Ampicillin (0–200 µg·mL<sup>-1</sup>). Cells were grown for 3.5 h at 37 °C with shaking and the A<sub>600 nm</sub> of cultures were determined.

### Screen for motile suppressors from the *flhA-K<sub>203A</sub>* variant

Cells of the *Salmonella flhA-K<sub>203A</sub>* strain were cultured at 37 °C in LB broth to mid-log phase and inoculated into soft tryptone agar (0.3% agar, 10 g·L<sup>-1</sup> tryptone, 5 g·L<sup>-1</sup> NaCl). Plates were incubated at 30 °C until motile ‘spurs’ appeared. Cells from the spurs were streaked to single colony and the *flhA* gene sequenced. New strains containing the *flhA-K<sub>203A</sub>* and suppressor mutations were constructed by aph-I-SceI λ Red recombination to confirm that the mutations within *flhA* were responsible for the motility suppressor phenotype [35].

### Quantification and statistical analysis

Experiments were performed at least three times. Immunoblot were quantified using Image Studio Lite. The unpaired two-tailed Student's *t*-test was used to determine *P*-values and significance was determined as \**P* < 0.05. Data are represented as mean ± standard error of the mean (SEM), unless otherwise specified and reported as biological replicates.

### Acknowledgements

This work was funded by a grant from the Biotechnology and Biological Sciences Research Council (BB/M007197/1) to GMF, and a University of Cambridge John Lucas Walker studentship to OJB.

### Conflict of interest

The authors declare no conflict of interest.

### Author contributions

OJB and GMF conceived and designed experiments. OJB conducted experiments. OJB analysed the data. OJB and GMF wrote the paper.

### Peer Review

The peer review history for this article is available at <https://publons.com/publon/10.1111/febs.16294>.

### Data availability statement

Materials are available from the corresponding authors upon request.

### References

- Deng W, Marshall NC, Rowland JL, McCoy JM, Worrall LJ, Santos AS, Strynadka NCJ & Finlay BB (2017) Assembly, structure, function and regulation of type III secretion systems. *Nat Rev Microbiol* **15**, 323–337.
- Galán JE, Lara-Tejero M, Marlovits TC & Wagner S (2014) Bacterial type III secretion systems: specialized nanomachines for protein delivery into target cells. *Annu Rev Microbiol* **68**, 415–438.
- Evans LDB, Hughes C & Fraser GM (2014) Building a flagellum outside the bacterial cell. *Trends Microbiol* **22**, 566–572.
- Evans LDB, Hughes C & Fraser GM (2014) Building a flagellum in biological outer space. *Microb Cell* **1**, 64–66.
- Kuhlen L, Abrusci P, Johnson S, Gault J, Deme JC, Caesar J, Dietsche T, Mebrhatu MT, Ganief T, Macek B *et al.* (2018) Structure of the core of the type III secretion system export apparatus. *Nat Struct Mol Biol* **25**, 583–590.
- Johnson S, Kuhlen L, Deme JC, Abrusci P & Lea SM (2019) The structure of an injectisome export gate demonstrates conservation of architecture in the core export gate between flagellar and virulence type III secretion systems. *MBio* **10**, e00818-19.
- Abrusci P, Vergara-Irigaray M, Johnson S, Beeby MD, Hendrixson D, Roversi P, Friede ME, Deane JE, Jensen GJ, Tang CM *et al.* (2012) Architecture of the major component of the type III secretion system export apparatus. *Nat Struct Mol Biol* **20**, 99–104.
- Saijo-Hamano Y, Imada K, Minamino T, Kihara M, Shimada M, Kitao A & Namba K (2010) Structure of the cytoplasmic domain of FlhA and implication for flagellar type III protein export. *Mol Microbiol* **76**, 260–268.
- Zarivach R, Vuckovic M, Deng W, Finlay BB & Strynadka NCJ (2007) Structural analysis of a

- prototypical ATPase from the type III secretion system. *Nat Struct Mol Biol* **14**, 131–137.
- 10 Imada K, Minamino T, Tahara A & Namba K (2007) Structural similarity between the flagellar type III ATPase FliI and F1-ATPase subunits. *Proc Natl Acad Sci USA* **104**, 485–490.
  - 11 Hu J, Worrall LJ, Vuckovic M, Hong C, Deng W, Atkinson CE, Finlay BB, Yu Z & Strynadka NCJ (2019) T3S injectisome needle complex structures in four distinct states reveal the basis of membrane coupling and assembly. *Nat Microbiol* **4**, 2010–2019.
  - 12 Kuhlen L, Johnson S, Zeitler A, Bäurle S, Deme JC, Caesar JE, Debo R, Fisher J, Wagner S & Lea SM (2020) The substrate specificity switch FlhB assembles onto the export gate to regulate type three secretion. *Nat Commun* **11**, 1296. <https://doi.org/10.1038/s41467-020-15071-9>
  - 13 Butan C, Lara-Tejero M, Li W, Liu J & Galán JE (2019) High-resolution view of the type III secretion export apparatus in situ reveals membrane remodeling and a secretion pathway. *Proc Natl Acad Sci USA* **116**, 24786–24795.
  - 14 Erhardt M, Wheatley P, Kim EA, Hirano T, Zhang Y, Sarkar MK, Hughes KT & Blair DF (2017) Mechanism of type-III protein secretion: regulation of FlhA conformation by a functionally critical charged-residue cluster. *Mol Microbiol* **104**, 234–249.
  - 15 Ibuki T, Imada K, Minamino T, Kato T, Miyata T & Namba KT (2011) Common architecture of the flagellar type III protein export apparatus and F- and V-type ATPases. *Nat Struct Mol Biol* **18**, 277–282.
  - 16 Kishikawa J, Ibuki T, Nakamura S, Nakanishi A, Minamino T, Miyata T, Namba KT, Konno H, Ueno H, Imada K *et al.* (2013) Common evolutionary origin for the rotor domain of rotary ATPases and flagellar protein export apparatus. *PLoS One* **8**, e64695.
  - 17 Minamino T, Morimoto Y, Hara N & Namba KT (2011) An energy transduction mechanism used in bacterial flagellar type III protein export. *Nat Commun* **2**, 475. <https://doi.org/10.1038/ncomms1488>
  - 18 Miletic S, Fahrenkamp D, Goessweiner-Mohr N, Wald J, Pantel M, Vesper O, Kotov V & Marlovits TC (2021) Substrate-engaged type III secretion system structures reveal gating mechanism for unfolded protein translocation. *Nat Commun* **12**, 1546. <https://doi.org/10.1038/s41467-021-21143-1>
  - 19 Bryant OJ, Dhillon P, Hughes C & Fraser GM (2020) Sequential recognition of discrete export signals in flagellar subunits during bacterial Type III secretion. *bioRxiv* <https://doi.org/10.1101/2020.12.09.414946>
  - 20 Hara N, Namba KT & Minamino T (2011) Genetic characterization of conserved charged residues in the bacterial flagellar type III export protein FlhA. *PLoS One* **6**, e22417.
  - 21 Ward E, Renault TT, Kim EA, Erhardt M, Hughes KT & Blair DF (2018) Type-III secretion pore formed by flagellar protein FliP. *Mol Microbiol* **107**, 94–103.
  - 22 Armbruster CE, Hodges SA, Smit SN, Alteri CJ & Mobley HLT (2014) Arginine promotes *Proteus mirabilis* motility and fitness by contributing to conservation of the proton gradient and proton motive force. *MicrobiologyOpen* **5**, 630–641.
  - 23 Minamino T, González-Pedrajo B, Kihara M, Namba KT & Macnab RM (2003) The ATPase FliI can interact with the type III flagellar protein export apparatus in the absence of its regulator, FliH. *J Bacteriol* **185**, 3983–3988.
  - 24 Minamino T & Namba KT (2008) Distinct roles of the FliI ATPase and proton motive force in bacterial flagellar protein export. *Nature* **451**, 485–488.
  - 25 Hughes KT, Gillen KL, Semon MJ & Karlinsey JE (1993) Sensing structural intermediates in bacterial flagellar assembly by export of a negative regulator. *Science* **262**, 1277–1280.
  - 26 Chilcott GS & Hughes KT (2000) Coupling of flagellar gene expression to flagellar assembly in *Salmonella enterica* Serovar Typhimurium and *Escherichia coli*. *Microbiol Mol Biol Rev* **64**, 694–708.
  - 27 Singer HM, Erhardt M & Hughes KT (2014) Comparative analysis of the secretion capability of early and late flagellar type III secretion substrates. *Mol Microbiol* **93**, 505–520.
  - 28 van den Berg B, Clemons WM Jr, Collinson I, Modis Y, Hartmann E, Harrison SC & Rapoport TA (2004) X-ray structure of a protein-conducting channel. *Nature* **427**, 36–44.
  - 29 Saparov SM, Erlandson K, Cannon K, Schaeletzky J, Schulman S, Rapoport TA & Pohl P (2007) Determining the conductance of the SecY protein translocation channel for small molecules. *Mol Cell* **26**, 501–509.
  - 30 Gumbart J & Schulte K (2008) The roles of pore ring and plug in the secY protein-conducting channel. *J Gen Physiol* **132**, 709–719.
  - 31 Minamino T, Morimoto YV, Hara N, Aldridge PD & Namba KT (2016) The bacterial flagellar Type III export gate complex is a dual fuel engine that can use both H<sup>+</sup> and Na<sup>+</sup> for flagellar protein export. *PLoS Pathog* **12**, e1005495.
  - 32 Minamino T, Kinoshita M, Inoue Y, Morimoto YV, Ihara K, Koya S, Hara N, Nishioka N, Kojima S, Homma M *et al.* (2016) FliH and FliI ensure efficient energy coupling of flagellar type III protein export in *Salmonella*. *Microbiol Open* **5**, 424–435.
  - 33 Bryant OJ, Chung BYW & Fraser GM (2021) Chaperone mediated coupling of subunit availability to activation of flagellar Type III Secretion. *Mol Microbiol* **116**, 538–549.
  - 34 Datsenko KA & Wanner BL (2000) One-step inactivation of chromosomal genes in *Escherichia coli*

- K-12 using PCR products. *Proc Natl Acad Sci USA* **97**, 6640–6645.
- 35 Hoffmann S, Schmidt C, Walter S, Bender JK & Gerlach RG (2017) Scarless deletion of up to seven methylaccepting chemotaxis genes with an optimized method highlights key function of CheM in *Salmonella* Typhimurium. *PLoS One* **12**, e0172630.
- 36 Amann E, Ochs B & Abel KJ (1988) Tightly regulated tac promoter vectors useful for the expression of unfused and fused proteins in *Escherichia coli*. *Gene* **69**, 301–315.
- 37 Miles AA, Misra SS & Irwin JO (1938) The estimation of the bactericidal power of the blood. *J Hyg (Lond)* **38**, 732–749.